Earth's Future

RESEARCH ARTICLE
10.1029/2020EF001803

Potential Influences of Volcanic Eruptions on Future Global Land Monsoon Precipitation Changes

Wenmin Man[1,2], Meng Zuo[1], Tianjun Zhou[1,2,3], John T. Fasullo[4], Ingo Bethke[5], Xiaolong Chen[1,2], Liwei Zou[1,2], and Bo Wu[1,2]

[1]LASG, Institute of Atmospheric Physics, Chinese Academy of Sciences, Beijing, China, [2]CAS Center for Excellence in Tibetan Plateau Earth Sciences, Chinese Academy of Sciences, Beijing, China, [3]University of Chinese Academy of Sciences, Beijing, China, [4]National Center for Atmospheric Research, Boulder, CO, USA, [5]Geophysical Institute, Bjerknes Centre for Climate Research, University of Bergen, Bergen, Norway

Key Points:

- The decadal-scale ensemble spread with realistic eruptions increases by 17.5% and 20.1% compared to no-volcanic and constant background-volcanic scenarios, respectively
- The centennial mean global land monsoon (GLM) precipitation was reduced by 10% with realistic eruptions, Asian monsoon region is the most impacted
- Volcanic activity could delay the time of emergence of anthropogenic influence by 5 years on average over about 60% of the GLM area

Supporting Information:

- Supporting Information S1

Correspondence to:
W. Man,
manwenmin@mail.iap.ac.cn

Citation:
Man, W., Zuo, M., Zhou, T., Fasullo, J. T., Bethke, I., Chen, X., et al. (2021). Potential influences of volcanic eruptions on future global land monsoon precipitation changes. *Earth's Future*, *9*, e2020EF001803. https://doi.org/10.1029/2020EF001803

Received 10 SEP 2020
Accepted 15 JAN 2021

Abstract The global monsoon system is of exceptional socioeconomic importance owing to its impacts on two-thirds of the globe's population. Major volcanic eruptions strongly influence global land monsoon (GLM) precipitation change. By using 60 plausible eruption scenarios sampled from reconstructed volcanic proxies over the past 2,500 years, 21st century volcanic influences on GLM precipitation projections are examined with an Earth system model under a moderate emission scenario. The decadal-scale ensemble spread with realistic eruptions (VOLC) increases by 17.5% and 20.1% compared to no-volcanic (NO-VOLC) and constant background-volcanic (VOLC-CONST) scenarios, respectively. Compared with NO-VOLC, the centennial mean VOLC GLM precipitation shows a 10% overall reduction and regionally, Asia is the most impacted. Changes in atmospheric circulation in the aftermath of large volcanic eruptions match the global warming response patterns well with opposite sign, with the North American monsoon precipitation enhanced following large volcanic eruptions, which is in sharp contrast to the robust decrease in Asian monsoon rainfall. Volcanic activity could delay the time of emergence of anthropogenic influence by five years on average over about 60% of the GLM area. Our results demonstrate the importance of statistical representation of potential volcanism for the projections of future monsoon variability. Quantifying volcanic impacts on regional climate projections and their socioeconomic influences on infrastructure planning, food security, and disaster management should be a priority of future work.

Plain Language Summary Understanding and predicting future global monsoon changes is critically important owing to its impacts on about two-thirds of population. Robust posteruption signals in the monsoon climate raise the question of their potential for a role in future climate. However, major volcanic eruptions are generally not included in current projection scenarios because they are inherently unpredictable events. By using 60 plausible eruption scenarios sampled from reconstructed volcanic proxies over the past 2,500 years, we revealed the volcanic impacts on the future changes of summer precipitation over global and submonsoon regions. Episodic volcanic forcing not only leads to a 10% overall reduction of the centennial global land monsoon (GLM) precipitation, but also causes larger ensemble spread (~20%) compared to no-volcanic and constant background-volcanic scenarios. Moreover, volcanic activity is projected to delay the time of emergence of anthropogenic GLM precipitation changes by five years on average over about 60% of the GLM area. Our results demonstrate the added value of incorporating major volcanic eruptions in monsoon projections.

1. Introduction

The global monsoon (GM) system can be described as the low latitude seasonal variation in precipitation and low-level winds and is of great socio-economic importance owing to its impacts on approximately two-thirds of the world's population (Trenberth & Dai, 2007; B. Wang & Ding, 2006). The monsoons are governed by a range of influences, including internal variability, natural external forcings, and human activities (P. Wang et al., 2014). Understanding and predicting these influences are critical for making informed decisions on mitigation and adaptation (W. Zhang et al., 2019).

Volcanic eruptions cause globally averaged surface temperature to cool and the hydrological cycle to weaken (Driscoll et al., 2012; Gillett et al., 2004; Grinsted et al., 2007; Timmreck, 2012). Global precipitation decreases are particularly pronounced in the year following large volcanic eruptions, as evidenced by paleoclimate reconstructions, historical observations, and climate model simulations (Anchukaitis et al., 2010; Colose et al., 2016; Gu et al., 2007; Iles & Hegerl, 2014, 2015; Schneider et al., 2009; Stevenson et al., 2016; Trenberth & Dai, 2007). Recent studies also indicate a pronounced regional and hemispheric redistribution of rainfall, characterized by monsoon weakening in the hemisphere of the eruption, and a strengthening in the opposing hemisphere (Fasullo et al., 2019; Zuo et al., 2019). A weakened monsoon circulation, caused by decreased land-ocean and interhemispheric thermal contrasts, enhance the rainfall decrease in the eruption hemisphere (Iles et al., 2013; Man et al., 2014; Zuo et al., 2019). These robust posteruption signals, involving interactions between the energy and water cycles, raise the question of their potential for a role in future climate (Santer et al., 2014).

However, major volcanic eruptions are generally not included in current climate projections because they are inherently unpredictable events. An earlier study examined the potential implications of a future eruption by setting a hypothetical Tambora eruption occurring in 2085, which demonstrated similar radiative responses as those during the 1815 event, however, a future eruption's peak response in both global mean temperature and rainfall is simulated to be approximately 40% greater than in 1815 through modulation of ocean stratification and near-surface winds (Fasullo et al., 2017). The Scenario Model Intercomparison Project (ScenarioMIP) of the Coupled Model Intercomparison Project Phase 6 (CMIP6), which will provide multimodel climate projections based on a range of scenarios of future emissions, specifies future volcanic forcing at a constant background value and thus does not account for future volcanic forcing variability, while the CMIP5 protocol optionally allowed specification of zero future volcanic forcing (O'Neill et al., 2016). In order to sample a more realistic range of volcanic forcing outcomes, Bethke et al. (2017) constructed a range of plausible eruption scenarios by sampling from reconstructed volcanic activity of the past 2,500 years (Sigl et al., 2015). By using these volcanic forcing scenarios under the middle-of-the-road scenario, that is representative concentration pathway (RCP) 4.5 (van Vuuren et al., 2011), they demonstrated that volcanic forcing uncertainty will likely have a significant impact on projected global temperature variance on interannual to interdecadal timescale and on the frequency of low temperature extremes. They also found increased projected precipitation variance over East Asia. However, responses in the global monsoon in such scenarios have yet to be explored in detail. In particular, the impacts from including plausible volcanic activity on projections of standard monsoon metrics, their regional and temporal variations and implications for the detection of anthropogenic signals are still unknown.

In this study, we investigate the influence of such forcing scenarios on projections of global land monsoon (GLM) precipitation by employing Norwegian Earth System Model (NorESM) projections under RCP4.5 (see Section 2.1). We quantify GLM precipitation changes and associated uncertainties across various periods and regions. We also perform a time of emergence (ToE) analysis (see Section 2.3) to address the volcanic impact on regional-scale shifts in the anthropogenic GLM precipitation changes relative to the background noise of internal variability. We show that the uncertainty range increases, and GLM precipitation decreases with the inclusion of realistic episodic volcanic forcing. Such information improves our understanding of future GLM precipitation changes.

It should be noted that our results are based on one single Earth System model, and there are also uncertainties from the coarse model resolution and the design of synthetic volcanic forcing. Coordinated multimodel efforts using the same plausible volcanic forcings should help us to reduce model uncertainties. Improved characterization of past volcanic forcing and its application to the model are both important for promoting the utilization of potential volcanism in future climate projections. All of these limitations and caveats of according results will be comprehensively discussed in this study.

2. Data and Methodology

2.1. Models and Data

The NorESM is one of the models that contributed to the Coupled Model Intercomparison Project Phase 5 (CMIP5) (Taylor et al., 2012). It was built upon the Community Climate System Model version 4 (CCSM4) but differs mainly in the implementation of an isopycnic coordinate ocean model and advanced chemistry-aerosol-cloud-radiation interaction schemes (Bentsen et al., 2013). NorESM1-M has a horizontal resolution of approximately 2° for the atmosphere and land components and 1° for the ocean and ice components. A large ensemble from a single climate model is a suitable tool to identify the role of external forcing relative to internal climate variability (Dai & Bloecker, 2019; Deser et al., 2012). In this study, we use three 60-member ensemble simulations spanning 2006–2099 with the NorESM1-M under different volcanic forcing: one ensemble using plausible episodic volcanic forcing (VOLC); one ensemble using zero volcanic forcing (NO-VOLC); and one ensemble using 1850–2000 averaged (i.e., background) volcanic forcing (VOLC-CONST). The simulations are the same as used by Bethke et al. (2017), with the notable difference that the VOLC-CONST ensemble has been enlarged from 20 to 60 members for this study. For the VOLC ensemble, Bethke et al. (2017) constructed 60 plausible volcanic forcing futures in terms of frequencies, magnitudes and geographic locations by utilizing the statistical representation of the past volcanic activity as reconstructed by Sigl et al. (2015) from a 2,500-year multiice-core record (Text S1).

While we cannot know the exact timing and magnitude of future eruptions, we do know that there will be episodic volcanic activity in the future and that this will tend to increase the level of natural climate variability as it has done in the past. Conventional climate projections are biased as they lack this source of variability. By utilizing synthetic volcanic forcing, we account for this variability source and by using an ensemble of outcomes we obtain a statistical representation of climate projection uncertainty related to the unknown future volcanic activity. The ensemble spreads of NO-VOLC and VOLC-CONST solely measure the contribution from internal climate variability to climate variance and projection uncertainty, whereas the ensemble spread of VOLC additionally reflects volcanic sourced climate variance and uncertainty. By comparing these experiments, we thus measure the volcanic contribution to natural climate variance and uncertainty against the level of unforced internal climate variability. There are additional uncertainties and sources of variance related to model representation, anthropogenic scenario and other natural forcings but their consideration is beyond the scope of this study.

2.2. Definition of Global Monsoon Domain

The global monsoon domains is defined by the regions where the local summer-minus-winter precipitation rate exceeds 2.0 mm day^{-1} and the local summer precipitation exceeds 55% of the annual total (B. Wang et al., 2012). The local summer is denoted as MJJAS (May through September) for the northern hemisphere (NH) and as NDJFM (November through March) for the southern hemisphere (SH). In this study, we define the global monsoon domain based on the 1979–2010 climatology from the Global Precipitation Climatology Project (GPCP) data version 2.2 (Huffman et al., 2009). The model could reasonably reproduce the global monsoon domain and global monsoon intensity (Figure S1). It can be further divided into seven monsoon subdomains (Kitoh et al., 2013). Since the global monsoon domain exists predominantly over land, we will focus on the influence of volcanic forcing on the local summer precipitation changes over the GLM domain.

2.3. ToE Analysis

The ToE is defined as the mean time at which the changes of GLM precipitation emerge from the noise of internal climate variability. To estimate ToE, we should first calculate "signal" and "noise" of the GLM precipitation (H. Zhang & Delworth, 2018). "Signal" is calculated as ensemble-mean, decadal-mean summer precipitation anomalies relative to the 1995–2014 mean over the GLM domain. Internal climate variability is estimated from the control simulation with a Monte Carlo approach at each grid point (Text S2). If the amplitude of the precipitation shift is outside the range of the internal climate variability, it is considered that the impact of human influences can be detected, and the corresponding period is called ToE. We will

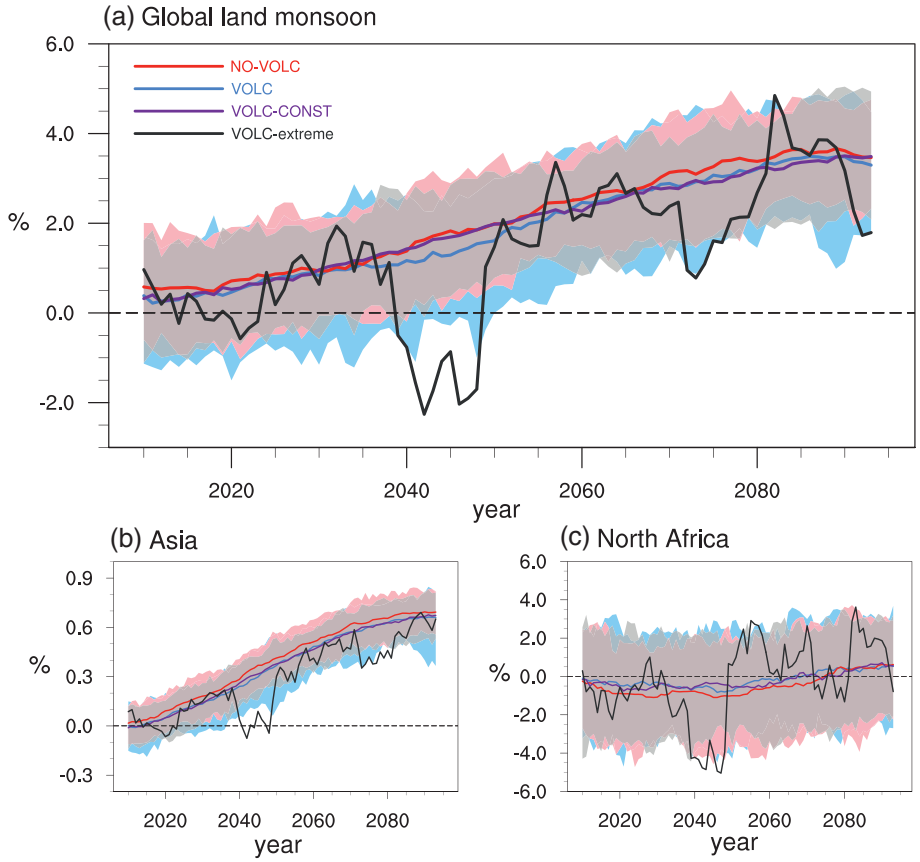

Figure 1. Time series of summer precipitation anomalies relative to the base period average (1995–2014) for the land monsoon domain (units: %) over (a) globe, (b) Asia, and (c) North Africa, expressed as percentage changes relative to the base period mean. The solid lines represent the ensemble mean of NO-VOLC (red), VOLC (blue), and VOLC-CONST (purple/gray) with the ensemble spread represented by 5–95 percentile of the ensemble member (shading); the black line denotes the evolution of the most extreme member with the peak centennially mean loadings. 10-year running mean was applied to all time series.

check the ToE change in VOLC relative to NO-VOLC to quantify the influence of episodic volcanic forcing on the ToE variability.

3. Results

3.1. Potential Volcanic Impacts on GLM Precipitation Projections

Time series of decadal summer precipitation anomalies over the GLM domain are displayed in Figure 1a. The ensemble mean from each simulation represents the externally forced response under RCP4.5, modified by a range of assumptions regarding volcanic forcing. These include the RCP4.5 scenario in which constant background aerosol concentrations are prescribed (VOLC-CONST), the RCP4.5 scenario with background aerosols removed (NO-VOLC), and a modified version of RCP4.5 in which stochastically generated eruptions are prescribed (VOLC). All the data are smoothed with a decadal smoother as here our focus is on low frequency volcanic impacts. The GLM precipitation ensemble mean (i.e. forced response, FR) experiences an overall increase in the 21st century under NO-VOLC. The effect of volcanic forcing on the GLM precipitation FR is modest, with the VOLC and VOLC-CONST being within the bounds of uncertainty of the FR. Compared with NO-VOLC (relative to base period mean), the centennial mean GLM precipitation change is reduced by 9.6% and 6.8% in VOLC and VOLC-CONST, respectively. Ensemble spread in VOLC, measured by 5–95 percentile of the ensemble member, gets 17.5% and 20.1% larger than that in NO-VOLC and VOLC-CONST, respectively. The uncertainty from volcanic forcing accounts for about 20% of the decadal-scale

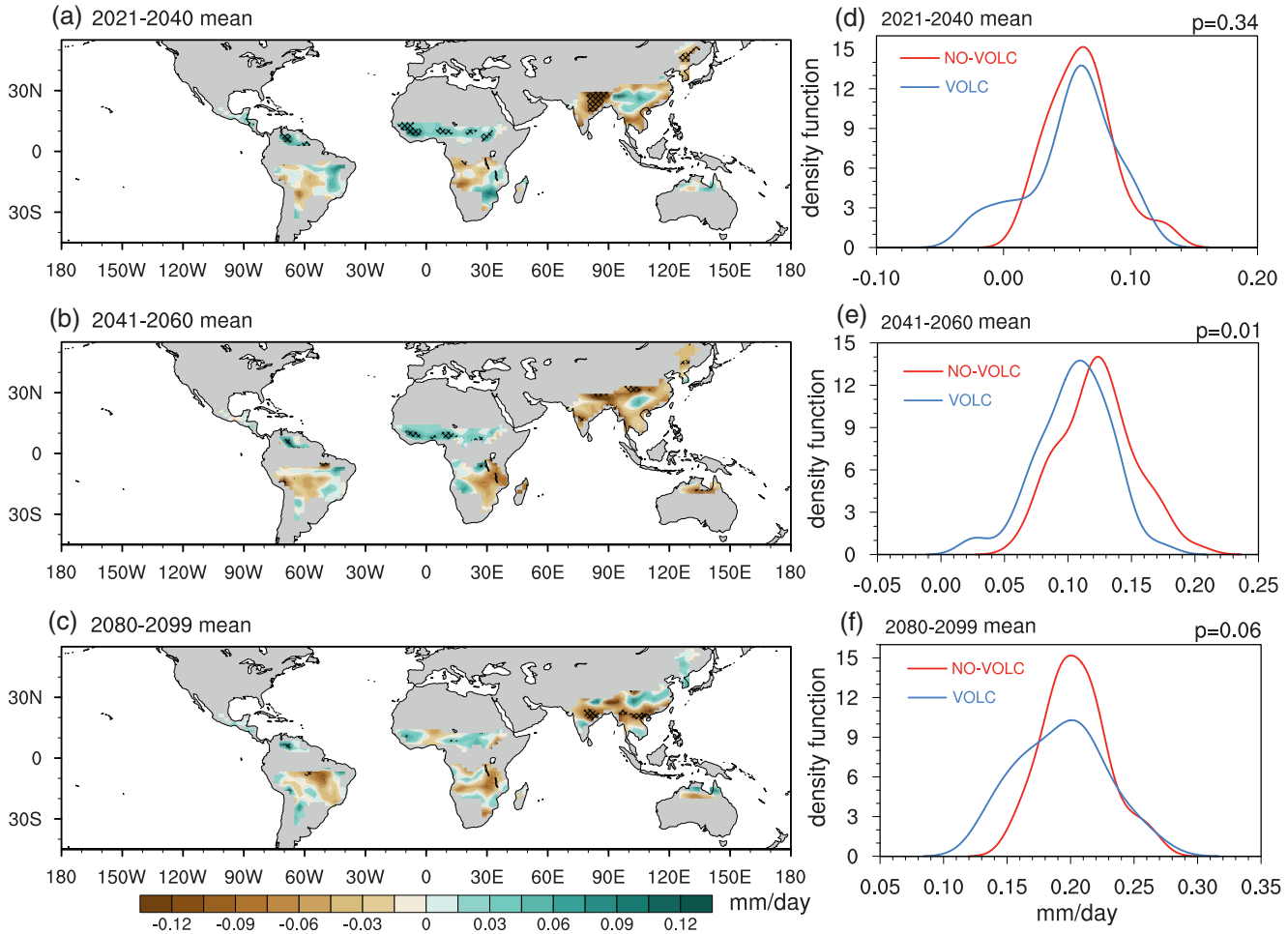

Figure 2. Precipitation difference between VOLC and NO-VOLC over the global land monsoon (GLM) domain (units: mm day^{-1}) in the (a) near-term (2021–2040), (b) mid-term (2041–2060), and (c) long-term (2081–2098) projection. The significance levels are determined according to the Student's-*t* test, and the slashes indicate the values that are statistically significant at the 5% level. The right panel represents probability density function (PDF) of the GLM precipitation for the (d) near-term (2021–2040), (e) mid-term (2041–2060), and (f) long-term (2081–2098) mean relative to the period 1995–2014. Red corresponds to NO-VOLC and blue corresponds to VOLC. Kernel density estimation is used to estimate all the PDFs. The Kolmogorov-Smirnov (KS) test is used to determine the significance of the PDF distributions. The PDF distribution of the GLM precipitation in VOLC and NO-VOLC is statistically distinguishable (KS test p values <0.05) for the mid-term projection.

internal climate variability in VOLC (Figure S2). This demonstrates that episodic volcanic forcing is a potentially important source of projection uncertainty that is not considered in the current ScenarioMIP of CMIP6 (Oneill et al., 2016). The associated impacts on precipitation in each monsoon subdomain are likely to be different, due to the influence of local dynamic and thermodynamic processes (Fischer et al., 2013; Ogorman, 2015). For example, as shown in Figures 1b and 1c, there is a marked contrast of the role of these forcing scenarios on the Asian and North African subdomains. In Asia, the reduction of the centennial precipitation change is 9.5% (6.1%–20.4%) in VOLC relative to NO-VOLC, whereas in North Africa, the strengthening of the centennial precipitation change is 64.5% (50.6%–76.0%).

To quantify the influence of episodic volcanic forcing on precipitation changes in different periods and regions, geographical distributions of precipitation changes are examined during three discrete intervals, termed the near-term (2021–2040), mid-term (2041–2060) and long-term (2081–2098), as summarized in Figure 2. The most significant volcanic influence on precipitation is the weakening of the Asian monsoon, and strengthening of the North African and North American monsoons (Figures 1b,1c, 2a and 2c). The presence of episodic volcanic forcing shifts the probability density function (PDF) distribution of the GLM precipitation, which is the spread across 60 ensemble members, to lower values in the mid- and long-term

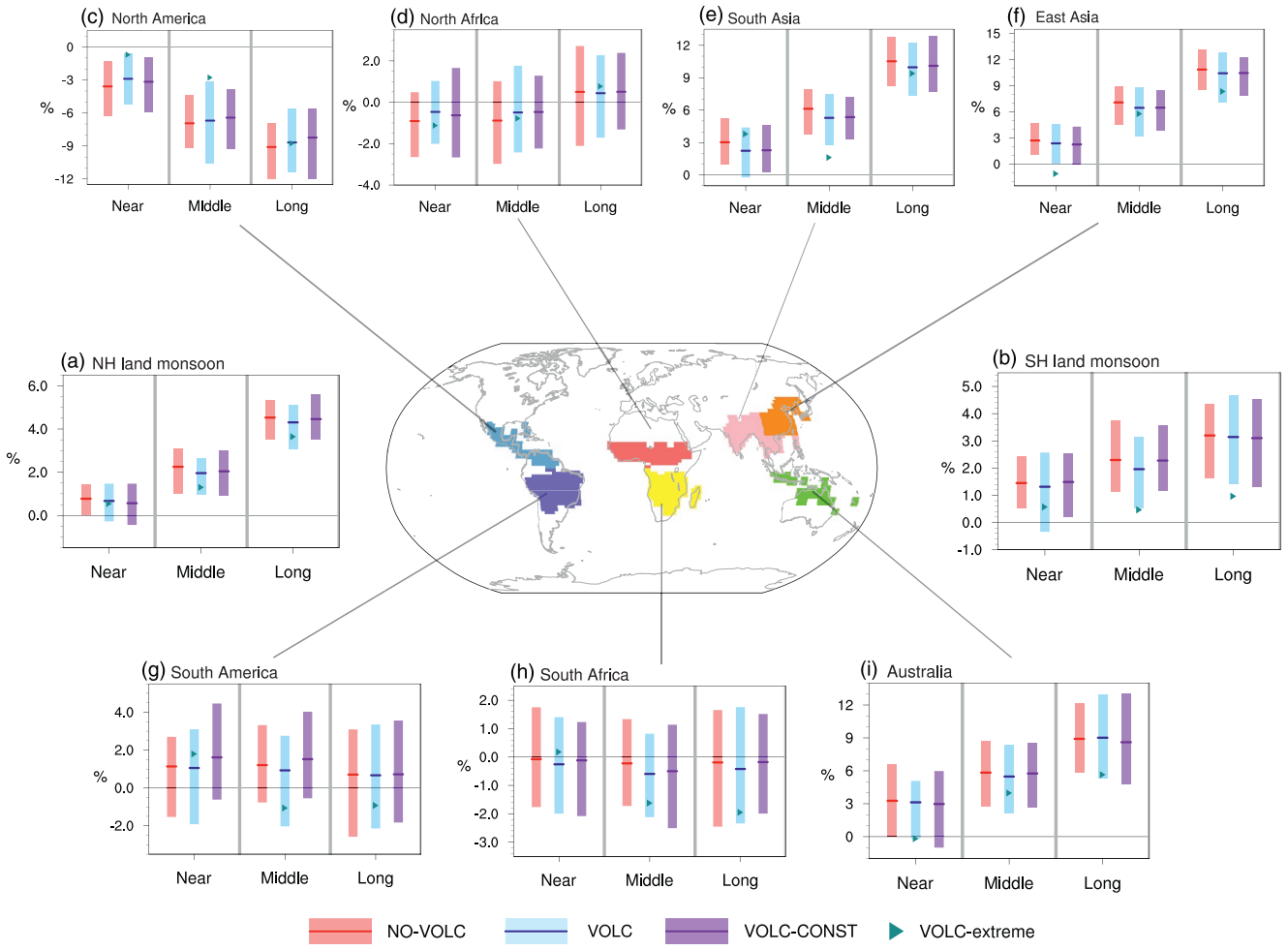

Figure 3. Summer precipitation changes over the NHLM and SHLM monsoon domain and each monsoon subdomain (units: %) three specific periods in future projection termed as the near-term (2021–2040), mid-term (2041–2060) and long-term (2081–2098) projection for NO-VOLC (red), VOLC (blue), and VOLC-CONST (purple) relative to the 1995–2014 mean. The thick lines represent the ensemble mean, while the bars indicate the uncertainty range measured by the 5–95 percentile of the ensemble member. The triangles denote the most extreme member. For region division, there are seven monsoon subdomains including North America, South America, North Africa, South Africa, South Asia, East Asia and Australia monsoon regions. The equator separates the northern monsoon domains from southern monsoon domains, and 20°N and 100°E separates South Asia from East Asia. NHLM and SHLM, northern and southern hemisphere land monsoon subdomains.

projections (Figures 2e and 2f), with considerably higher significance than for near-term projections (Figure 2d). To the extent that the volcanic forcing history during the observed period has an influence on the 2021–2040 projections via ocean memory effects, which is the same for all experiments, we could expect to see a smaller response for the near-term compared to mid-term and long-term. The mid-term versus long-term differences in the PDF shapes for VOLC are likely due to both sampling and background state dependence. The PDF distribution also shifts to lower values with the inclusion of episodic volcanic forcing than that of background volcanic forcing (Figure S3).

We further define seven monsoon subdomains in the vicinity of North America, South America, North Africa, South Africa, South Asia, East Asia, and Australia. Figures 3a and 3b show summer precipitation changes in the northern and southern hemisphere land monsoon subdomains (NHLM and SHLM, respectively) and in each subdomain over near-, mid-, and long-term intervals. The uncertainty range represented by 5%–95% ensemble spread for the 20-year mean is shown for the bars. The triangles denote the most extreme member, which is ranked by the centennially mean aerosol loadings, thus may contain a Samalas type of eruption and some other large eruptions. The model projects an enhancement of NHLM and SHLM precipitation across all time intervals under RCP4.5. The projected increase of NHLM precipitation is larger

than that of SHLM, while the ensemble spread is larger for the SHLM than the NHLM. These features are comparable to those in CMIP5 projections simulated for RCP4.5 (Kitoh et al., 2013; Lee & Wang, 2014). The increase of monsoon precipitation in the mid-term projection is most affected by the volcanic forcing. Compared with NO-VOLC, the precipitation increase in VOLC is reduced by 8.3% (4.6%–17.0%) and 11.2% (5.1%–28.1%) over the NHLM and SHLM domains, respectively. Extremely strong volcanic activity could cause much larger precipitation variability as evident in the most extreme member. Such outlier behavior is nonetheless important for adequate risk assessments on hydrologic extremes and impacts in a warming climate. However, the application of background volcanic forcing would fail to capture the extreme response to episodic volcanic forcing. More quantified results are shown in Table S1.

For monsoon subdomains, precipitation increases over North Africa, Asia, and Australia across timescales (Figures 3d–3f, and 3i), but slightly decreases over North America, South America and South Africa (Figures 3c, 3g, and 3h), due to the interhemispheric difference under RCP4.5. The inclusion of either background or episodic volcanic forcing results in decreased precipitation on average over most monsoon subdomains from near-term to long-term except North America and North Africa (Figures 3c and 3d). The decrease in the South Asian and East Asian monsoon domain is the most robust relative to internal variability, as demonstrated by the magnitude of the signal-to-noise ratio shown in Table S2. It should be noted that this finding might be slightly model dependent. Moreover, the ensemble spread is enhanced in VOLC relative to NO-VOLC and VOLC-CONST over most monsoon subdomains.

3.2. Atmospheric Circulation Changes in the Aftermath of Large Volcanic Eruptions

In addition to the potential volcanic impacts on GLM precipitation projections and associated uncertainties based on the ensemble of simulations, it would be good to include some more physical background considerations, such as changes in atmospheric circulation in the aftermath of large volcanic eruptions and how they compare to future changes in monsoon in response to global warming. The advantage of assessing changes in atmospheric circulation is that large-scale changes are less sensitive to local conditions. Also changes in precipitation which are challenging to simulate by coarse-scale global climate models are more robust in relation to atmospheric circulation.

The responses of monsoon circulation that followed the large volcanic eruptions are shown in Figure 4. The eruptions whose stratospheric sulfate aerosol loading exceeds 30 Terrogram (Tg) are selected from the 60-member future forcing time series. The year in which the volcanic aerosol mass peaks is regarded as year 0, and the following year is named as year 1. We focus on the responses in the first local summer (MJJAS of year 1 for the NH monsoon region; November and December (year 0) and January–March (year 1) for the SH monsoon region), which is calculated with respect to a 5-year preeruption mean (Iles et al., 2013). The composite volcanic response patterns match the global warming response patterns well with opposite sign (Figure S4). It makes sense since the first-order large-scale volcanic climate impact is a surface cooling while the global warming predominantly warms the surface. For the Asian monsoon region, both the southwesterlies from the Indian monsoon and the southeasterlies from the western Pacific are negative, which correspond to a weakened Asian monsoon circulation and reduced precipitation following large volcanic eruptions. The North American monsoon precipitation enhances corresponding to an anomalous cyclonic circulation, in sharp contrast to the robust decrease in Asian monsoon rainfall. The monsoon circulations over the South American, South African, and Australian monsoon regions exhibit anticyclonic anomalies in the aftermath of large volcanic eruptions, which lead to significant decrease of monsoonal precipitation in their warm seasons. These results are comparable to the drying effects of past eruptions in the regional monsoons, mainly through the monsoon circulation weakening resulting from reduced land-sea thermal contrast (Colose et al., 2016; Cui et al., 2014; Dogar & Sato, 2019; Dogar et al., 2017; Gao et al., 2018; Man et al., 2014; Wegmann et al., 2014; Zambri et al., 2017; Zhuo et al., 2020). The increased precipitation over the North American monsoon region is possibly due to precipitation decrease of the Intertropical Convergence Zone (ITCZ) and an anticyclone anomaly over the Eurasian-African continental area after the strong volcanic forcing, which lead to anomalous ascending motion and enhanced North American monsoon rainfall (Figures S5 and S6). This matches the mechanism that claimed for the drier North American monsoon

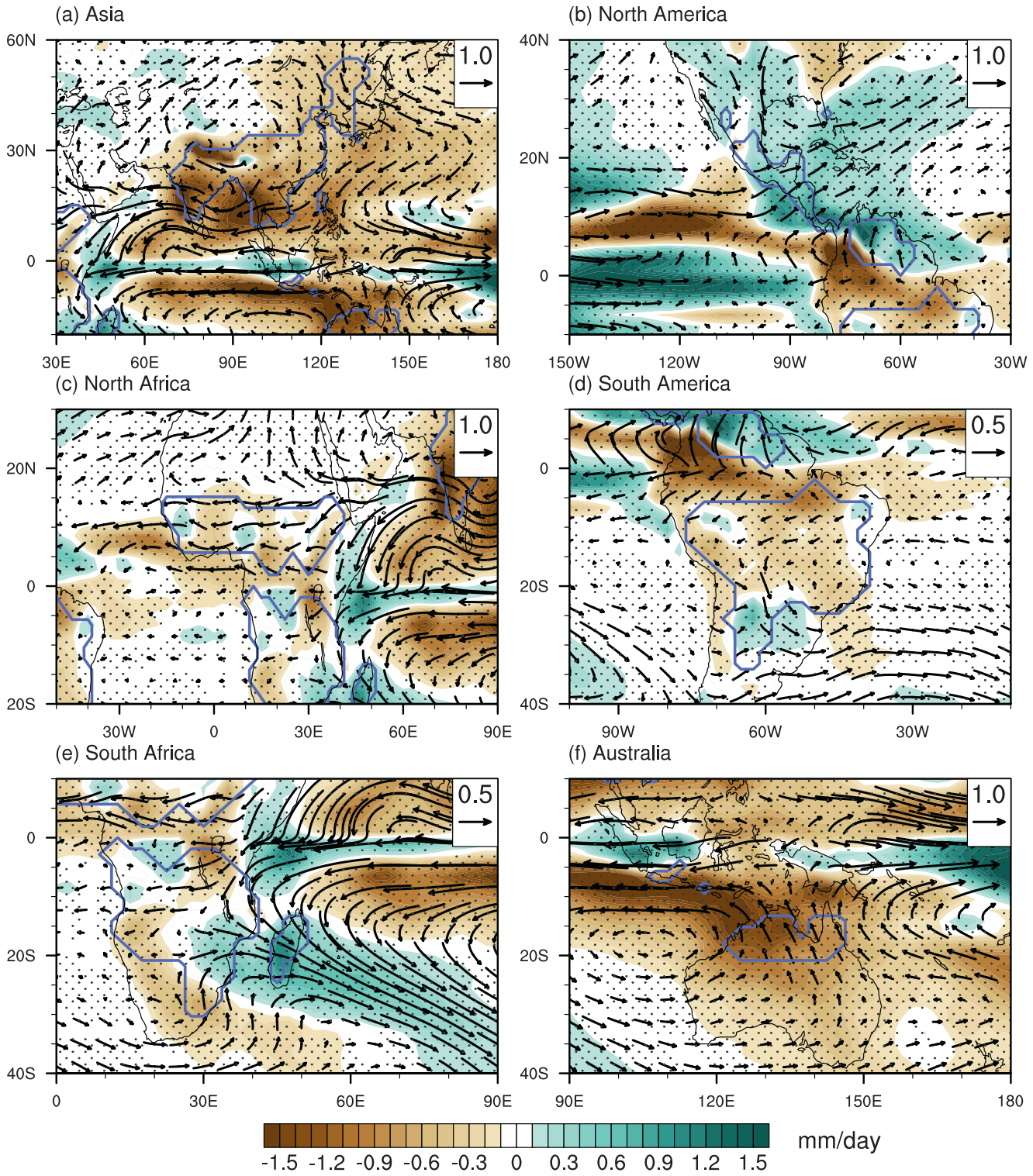

Figure 4. Composite analysis of 850-hPa wind (vectors; m s^{-1}) and precipitation (shading; mm day^{-1}) anomalies in the local summer of year 0 and year 1 (MJJAS of year 1 for the NH monsoon region; November and December (year 0) and January–March (year 1) for the SH monsoon region) following the large volcanic eruptions. The anomalies are calculated with respect to a 5-year preeruption mean. Dots denote areas that are significant at the 5% level derived from 1,000 Monte Carlo simulations.

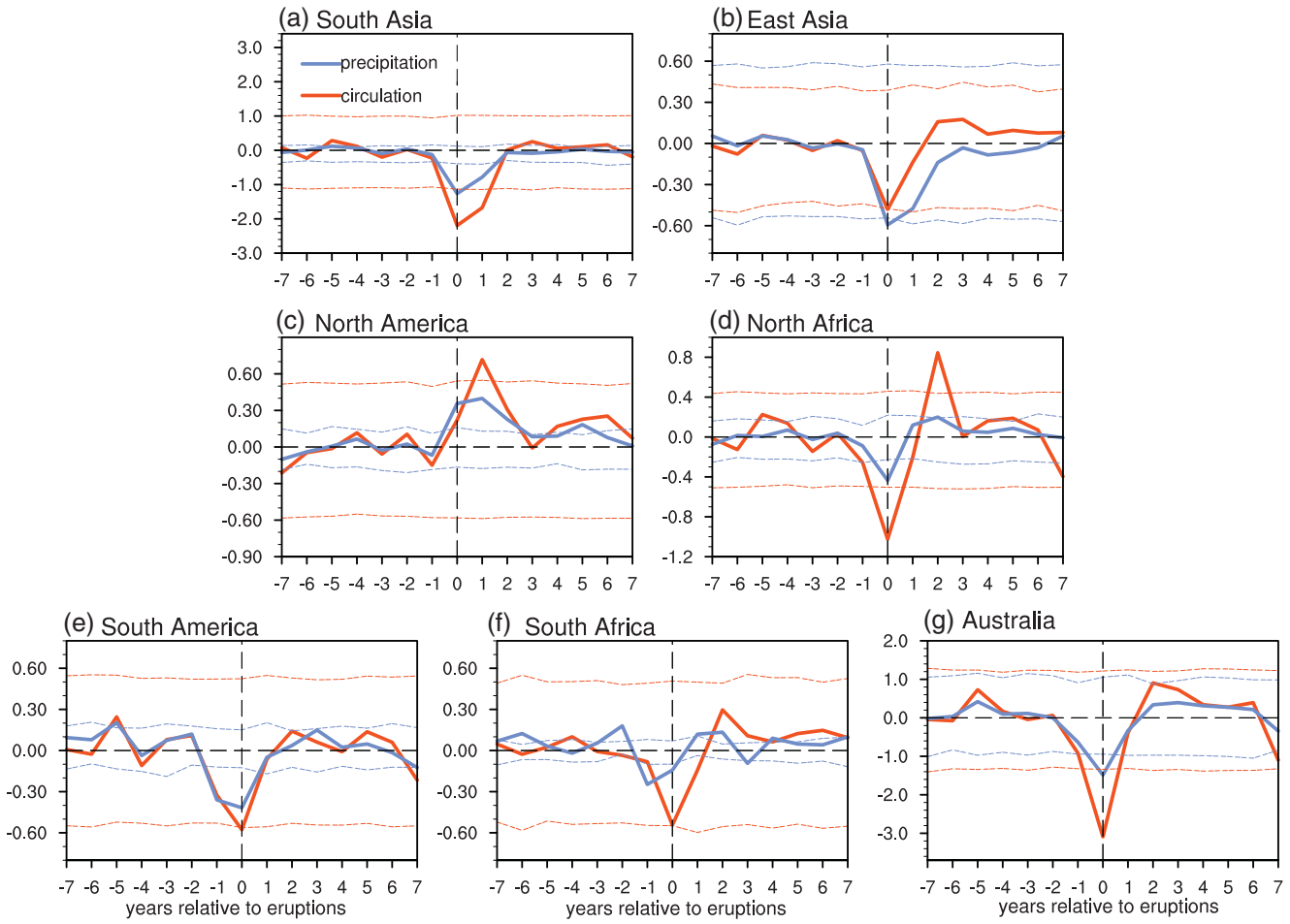

Figure 5. Summer monsoon precipitation and low-level circulation responses averaged across the large volcanic eruptions: (a) South Asia, (b) East Asia, (c) North America, (d) North Africa, (e) South America, (f) South Africa, and (g) Australia monsoon regions. Dashed lines represent confidence intervals of 95% derived from 1,000 Monte Carlo simulations.

under global warming, with the response caused by strong volcanic forcing completely opposite to the fast response caused by the increased CO_2 concentration (He et al., 2020).

The temporal patterns of monsoon circulation and precipitation averaged across the large volcanic eruptions are further assessed by using the superposed epoch analysis (SEA) method (Haurwitz & Brier, 1981) (Figure 5). The circulation indices are defined for each regional monsoon as in Jin et al. (2020), with the enhanced regional monsoon precipitation commonly characterized by a low-level cyclonic circulation. There is a peak monsoon weakening during the volcanic eruption year and one year after in each monsoon region except the North American monsoon. The corresponding precipitation significantly decreases in the eruption year and the first aftermath year, and returns to normal conditions thereafter. This temporal developments of monsoon indices and precipitation further confirm that the dynamic response via monsoon circulation weakening can be a critical factor for precipitation reduction to volcanic forcing (Joseph & Zeng, 2011; Paik & Min, 2017).

3.3. Volcanic Influence on ToE of Anthropogenic GLM Precipitation Changes

The ToE difference between VOLC and NO-VOLC is further assessed to quantify its sensitivity to volcanic forcing (Figure 6). The result shows a small but identifiable influence of volcanic forcing prescription on ToE (Figure 6a). The ToE, defined as the mean time at which the changes of GLM precipitation emerge from

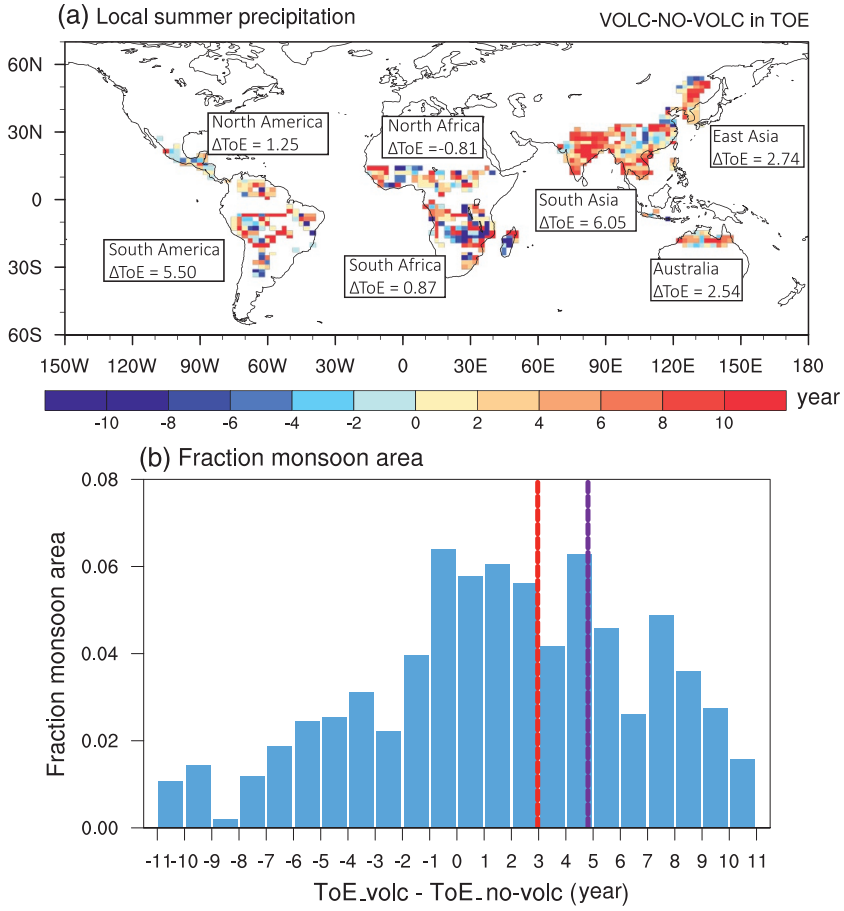

Figure 6. Time of emergence (ToE) of anthropogenic GLM precipitation changes (units: year). (a) ToE difference between VOLC and NO-VOLC relative to 1995–2014 mean. (b) Fraction monsoon area of ToE difference between VOLC and NO-VOLC, with dashed lines denoting mean ToE averaged over the whole monsoon region (red) or monsoon region with delayed ToE (purple).

the noise of internal climate variability, is delayed over a large part of the GLM domain in VOLC relative to NO-VOLC. As expected, the most distinguishable delay occurs mainly in the Asian monsoon region, where the regional decrease in precipitation is the largest. However, in certain location, such as the North African monsoon, the model projects a shift to an earlier emergence, indicating the moistening influence of episodic eruptions in this region. The distribution of the simulated delay is skewed, with about 60% of the GLM domain shifting to a later timing (Figure 6b). The delays are three years when considered over the whole monsoon region, and five years when considered over only those monsoon regions with delayed ToE. Delays up to a decade are estimated in some locations, however, such as South Asia. Compared with background volcanic forcing, episodic volcanic activity causes only a marginal change in ToE over the whole GLM region (Figure S7).

4. Summary and Discussion

In summary, we explore the effects of stochastically generated episodic volcanic forcing on precipitation projections for the global monsoon. Realistic eruptions are found to influence ensemble spread and associated uncertainties, an effect that has yet to be accounted for in most projections of GLM precipitation. Ensemble projections of GLM precipitation decrease in the mid- and late-21st C relative simulations without volcanic aerosols. Episodic volcanic forcing is also projected to cause distinguishable ToE delays of at least five years in over 60% of the GLM domain. These results demonstrate the value of incorporating more

realistic volcanic eruptions in climate projections in order to better quantify the evolving ensemble distribution. Our results also suggest that climate models that do not use realistic volcanic forcing introduce an associated systematic bias in their ensemble projections.

This study entails various caveats, which include the general problems in simulating precipitation with a coarsely resolved climate model, effects of ensemble size on statistical robustness, large interregional spatial variability in the ToE metric, the model dependency of these findings and uncertainties in estimates of future volcanic forcing scenarios. Coarse resolution climate models are limited in their ability to resolve aspects of regional precipitation due to coarsely resolved topography and limited vertical resolution in the lower troposphere (Haarsma et al., 2016; Mishra et al., 2018; Yang et al., 2019). These shortcomings are known to impact regional features of the precipitation distribution and its response to forcing. Other aspects however, such as land-ocean contrasts and simulated increase in ensemble spread in large-scale precipitation metrics are less sensitive to such effects, as they are rooted in energetically constrained responses (Fasullo et al., 2019) and thermodynamic contrasts between land and ocean (Fasullo, 2012).

When considering regional precipitation responses over 20-year time periods, large simulation ensembles with many volcanic forcing evolutions are needed to sufficiently sample potential volcanism and robustly detect responses in the presence of large regional internal climate variability, partly related to ENSO (Paik et al., 2020). Increasing the ensemble size beyond 60 would likely improve consistency in our results for the individual monsoon regions.

Despite a general tendency toward delayed ToE with episodic volcanic forcing, opposite changes are found at many grid points in the monsoon subdomains with the possible exception of some of South and East Asia. This is because the precipitation change signal extracted at the local scale may be influenced by internal variability or other noise. The uncertainties from internal climate variability are essentially irreducible at the local scale (Fischer et al., 2013). We refer to the multimember mean as an estimate of the forced signal, that is, the response to the imposed forcing in the absence of variability. The departures from this forced signal arise from internal variability inherent to the coupled climate system. The effect of internal variability generally decreases if variables are averaged across region or the globe (Fischer et al., 2013). Thus, our estimate of regional ToE is robust and less affected by internal variability. The aggregated spatial probability perspective provides a new method to improve the weakness of the projection agreement at the grid-point level.

Model dependency of the climate response to a given volcanic forcing is another concern. While the model's global temperature response to the 1991 Pinatubo eruption exhibits to agree with other model and observational estimates (Bethke et al., 2017), it is challenging to verify the model's precipitation response without established benchmarks to compare with. Consistent with proxy and other model studies (Liu et al., 2016; Zambri & Robock, 2016), our model produces posteruption precipitation decreases that are particularly pronounced over the Asian monsoon region (Figure 4). To further address intermodel uncertainties in regional monsoon responses would require comparing multiple models with the same volcanic forcing. The Model Intercomparison Project on the Climatic Response to Volcanic Forcing (VolMIP) that has been endorsed by CMIP6 provides a platform for coordinating the multimodel efforts currently underway to better understand these and related questions (Zanchettin et al., 2016).

Other uncertainties arise from the volcanic forcing and its application to the model. The scaling of stratospheric aerosol loads to sulfate peaks in ice cores introduces error due to nonuniform surface deposition (Gao et al., 2007), which is partly mitigated by the use of spatially separated multiice-core records (Sigl et al., 2013, 2015). Ice core reconstructions generally omit the effects of small eruptions and the differential deposition between Greenland and Antarctica allows only a crude spatial characterization of past explosive volcanism (Text S1) and provides no information on seasonality and duration. The use of prescribed concentrations in the simulations with three generic evolutions (Figure S9) oversimplifies the spatiotemporal dispersion of volcanic aerosols (Bethke et al., 2017), introduces particle size related forcing errors (Lacis, 2015) and neglects reduced efficiency under global warming of volcanic sulfate reaching the stratosphere (Aubry et al., 2016). The resampling approach by Bethke et al. (2017) produces eruption frequencies that resemble those of the reconstructed variability, but their representativeness beyond the reconstruction period is poor for the largest eruptions that occur rarely (e.g., the 2,500-year period features only two Samalas-size

eruptions). Ammann and Naveau (2010) address this with a more advanced method for producing stochastic volcanic forcing, based on distribution fitting and extreme value theory, that should be considered for future studies.

In summary, these uncertainties will likely not change our main conclusions, and they nevertheless highlight the need for similar studies with different models and improved future volcanic forcing characterization and implementation to better assess potential future volcanic effects on regional monsoon projections. Improved representation of future volcanic forcing variability and coordinated multimodel comparisons are thus essential ingredients to reliable future climate projections with a complete representation of uncertainties.

Data Availability Statement

The NorESM ensemble output from 21st century experiments with stochastic volcanic forcing, zero volcanic forcing, and constant volcanic forcing were acquired from https://doi.org/10.11582/2017.00006.

Acknowledgments
This work is jointly supported by the National Natural Science Foundation of China (Grants No. 41675802, 42075041), the National Program on Key Basic Research Project of China (Grants 2017YFA0604601, 2020YFA0608902), the International Partnership Program of the Chinese Academy of Sciences (Grant 134111KYSB20160031), the Second Tibetan Plateau Scientific Expedition and Research (STEP) program (Grant No. 2019QZKK0102), and the Jiangsu Collaborative Innovation Center for Climate Change. The efforts of Dr. Fasullo in this work were supported by NASA Award 80NSSC17K0565, by NSF Award #AGS-1419571, and by the Regional and Global Model Analysis (RGMA) component of the Earth and Environmental System Modeling Program of the U.S. Department of Energy's Office of Biological & Environmental Research (BER) via National Science Foundation IA 1844590. Dr. Ingo Bethke was supported by the Trond Mohn Foundation through the Bergen Climate Prediction Unit (BCPU, Grant BFS2018TMT01). CPU and storage was provided by UNINETT Sigma2 (nn9039k, ns9039k).

References

Ammann, C. M., & Naveau, P. (2010). A statistical volcanic forcing scenario generator for climate simulations. *Journal of Geophysical Research*, *115*, D05107. https://doi.org/10.1029/2009jd012550

Anchukaitis, K. J., Buckley, B. M., Cook, E. R., Cook, B. I., D'Arrigo, R. D., & Ammann, C. M. (2010). Influence of volcanic eruptions on the climate of the asian monsoon region. *Geophysical Research Letters*, *37*, L22703. https://doi.org/10.1029/2010gl044843

Aubry, T. J., Jellinek, A. M., & Degruyte, W. (2016). Impact of global warming on the rise of volcanic plumes and implications for future volcanic aerosol forcing. *Journal of Geophysical Research: Atmospheres*, *121*(13), 13326–13351. https://doi.org/10.1002/2016JD025405

Bentsen, M., Bethke, I., Debernard, J. B., Iversen, T., Kirkevag, A., Seland, O., et al. (2013). The Norwegian earth system model, noresm1-m—Part 1: Description and basic evaluation of the physical climate. *Geoscientific Model Development*, *6*(3), 687–720. https://doi.org/10.5194/gmd-6-687-2013

Bethke, I., Outten, S., Otterå, O. H., Hawkins, E., Wagner, S., Sigl, M., & Thorne, P. (2017). Potential volcanic impacts on future climate variability. *Nature Climate Change*, *7*(11), 799–805. https://doi.org/10.1038/nclimate3394

Colose, C. M., LeGrande, A. N., & Vuille, M. (2016). The influence of volcanic eruptions on the climate of tropical South America during the last millennium in an isotope-enabled general circulation model. *Climate of the Past*, *12*(4), 961–979. https://doi.org/10.5194/op-12-961-2016

Cui, X. D., Gao, Y. Q., & Sun, J. Q. (2014). The response of the East Asian summer monsoon to strong tropical volcanic eruptions. *Advances in Atmospheric Sciences*, *31*(6), 1245–1255. https://doi.org/10.1007/s00376-014-3239-8

Dai, A., & Bloecker, C. E. (2019). Impacts of internal variability on temperature and precipitation trends in large ensemble simulations by two climate models. *Climate Dynamics*, *52*(1–2), 289–306. https://doi.org/10.1007/s00382-018-4132-4

Deser, C., Knutti, R., Solomon, S., & Phillips, A. S. (2012). Communication of the role of natural variability in future north American climate. *Nature Climate Change*, *2*(11), 775–779. https://doi.org/10.1038/nclimate1562

Dogar, M., & Sato, T. (2019). Regional climate response of Middle Eastern, African, and South Asian monsoon regions to explosive volcanism and ENSO forcing. *Journal of Geophysical Research: Atmospheres*, *124*, 7580–7598. https://doi.org/10.1029/2019JD030358

Dogar, M., Stenchikov, G., Osipov, S., Wyman, B., & Zhao, M. (2017). Sensitivity of the regional climate in the Middle East and North Africa to volcanic perturbations. *Journal of Geophysical Research: Atmospheres*, *122*, 7922–7948. https://doi.org/10.1002/2017JD026783

Driscoll, S., Bozzo, A., Gray, L. J., Robock, A., & Stenchikov, G. (2012). Coupled model intercomparison project 5 (CMIP5) simulations of climate following volcanic eruptions. *Journal of Geophysical Research*, *117*, D17105. https://doi.org/10.1029/2012jd017607

Fasullo, J. T. (2012). A Mechanism for land-ocean contrasts in global monsoon trends in a warming climate. *Climate Dynamics*, *39*, 1137–1147. https://doi.org/10.1007/s00382-011-1270-3

Fasullo, J. T., Otto-Bliesner, B. L., & Stevenson, S. (2019). The influence of volcanic aerosol meridional structure on monsoon responses over the last millennium. *Geophysical Research Letters*, *46*(21), 12350–12359. https://doi.org/10.1029/2019gl084377

Fasullo, J. T., Tomas, R., Stevenson, S., Otto-Bliesner, B., Brady, E., & Wahl, E. (2017). The amplifying influence of increased ocean stratification on a future year without a summer. *Nature Communications*, *8*, 1236. https://doi.org/10.1038/s41467-017-01302-z

Fischer, E. M., Beyerle, U., & Knutti, R. (2013). Robust spatially aggregated projections of climate extremes. *Nature Climate Change*, *3*(12), 1033–1038. https://doi.org/10.1038/nclimate2051

Gao, C. C., & Gao, Y. J. (2018). Revisited Asian monsoon hydroclimate response to volcanic eruptions. *Journal of Geophysical Research: Atmospheres*, *123*, 7883–7896. https://doi.org/10.1029/2017JD027907

Gao, C. C., Oman, L., Robock, A., & Stenchikov, G. L. (2007). Atmospheric volcanic loading derived from bipolar ice cores accounting for the spatial distribution of volcanic deposition. *Journal of Geophysical Research: Atmospheres*, *112*, D09109. https://doi.org/10.1029/2006JD007461

Gillett, N. P., Weaver, A. J., Zwiers, F. W., & Wehner, M. F. (2004). Detection of volcanic influence on global precipitation. *Geophysical Research Letters*, *31*(12), L12217. https://doi.org/10.1029/2004gl020044

Grinsted, A., Moore, J. C., & Jevrejeva, S. (2007). Observational evidence for volcanic impact on sea level and the global water cycle. *Proceedings of the National Academy of Sciences of the United States of America*, *104*(50), 19730–19734. https://doi.org/10.1073/pnas.0705825104

Gu, G., Adler, R. F., Huffman, G. J., & Curtis, S. (2007). Tropical rainfall variability on interannual-to-interdecadal and longer time scales derived from the GPCP monthly product. *Journal of Climate*, *20*, 4033–4046. https://doi.org/10.1175/JCLI4227.1

Haarsma, R. J., Roberts, M. J., Senior, C. A., Belluci, A., Bao, Q., Chang, P., et al. (2016). High Resolution Model Intercomparison Project (HighResMIP v1.0) for CMIP6. *Geoscientific Model Development*, *9*, 4185–4208. https://doi.org/10.5194/gmd-9-4185-2016

Haurwitz, M. W., & Brier, G. W. (1981). A critique of the superposedepoch analysis method: Its application to solar-weather relations. *Monthly Weather Review*, *109*, 2074–2079. https://doi.org/10.1175/1520-0493(1981)109,2074:ACOTSE.2.0.CO;2

He, C., Li, T., & Zhou, W. (2020). Drier North American monsoon in contrast to Asian-African monsoon under global warming. *Journal of Climate*, *33*, 9801–9816. https://doi.org/10.1175/JCLI-D-20-0189.1

Huffman, G. J., Adler, R. F., Bolvin, D. T., & Gu, G. (2009). Improving the global precipitation record: GPCP version 2.1. *Geophysical Research Letters*, *36*, L17808. https://doi.org/10.1029/2009gl040000

Iles, C. E., & Hegerl, G. C. (2014). The global precipitation response to volcanic eruptions in the CMIP5 models. *Environmental Research Letters*, *9*(10), 104012. https://doi.org/10.1088/1748-9326/9/10/104012

Iles, C. E., & Hegerl, G. C. (2015). Systematic change in global patterns of streamflow following volcanic eruptions. *Nature Geoscience*, *8*(11), 838–842. https://doi.org/10.1038/ngeo2545

Iles, C. E., Hegerl, G. C., Schurer, A. P., & Zhang, X. (2013). The effect of volcanic eruptions on global precipitation. *Journal of Geophysical Research: Atmospheres*, *118*(16), 8770–8786. https://doi.org/10.1002/jgrd.50678

Jin, C. H., Wang, B., & Liu, J. (2020). Future changes and controlling factors of the eight regional monsoons projected by CMIP6 models. *Journal of Climate*, *33*, 9307–9326. https://doi.org/10.1175/JCLI-D-20-0236.1

Joseph, R., & Zeng, N. (2011). Seasonally modulated tropical drought induced by volcanic aerosol. *Journal of Climate*, *24*, 2045–2060. https://doi.org/10.1175/2009JCLI3170.1

Kitoh, A., Endo, H., Kumar, K. K., Cavalcanti, I. F. A., Goswami, P., & Zhou, T. (2013). Monsoons in a changing world: A regional perspective in a global context. *Journal of Geophysical Research: Atmospheres*, *118*(8), 3053–3065. https://doi.org/10.1002/jgrd.50258

Lacis, A. (2015). Volcanic aerosol radiative properties. *PAGES Magazine*, *23*(2), 50–51. https://doi.org/10.22498/pages.23.2.50

Lee, J.-Y., & Wang, B. (2014). Future change of global monsoon in the cmip5. *Climate Dynamics*, *42*(1–2), 101–119. https://doi.org/10.1007/s00382-012-1564-0

Liu, F., Chai, J., Wang, B., Liu, J., Zhang, X., & Wang, Z. (2016). Global monsoon precipitation responses to large volcanic eruptions. *Scientific Reports*, *6*, 24331. https://doi.org/10.1038/srep24331

Man, W., Zhou, T., & Jungclaus, J. H. (2014). Effects of large volcanic eruptions on global summer climate and east Asian monsoon changes during the last millennium: Analysis of MPI-ESM simulations. *Journal of Climate*, *27*(19), 7394–7409. https://doi.org/10.1175/jcli-d-13-00739.1

Mishra, S. K., Sahany, S., Salunke, P., Kang, I.-S., & Jain, S. (2018). Fidelity of CMIP5 multi-model mean in assessing Indian monsoon simulations. *npj Climate and Atmospheric Science*, *1*, 39. https://doi.org/10.1038/s41612-018-0049-1

O'Gorman, P. A. (2015). Precipitation extremes under climate change. *Current Climate Change Reports*, *1*, 49–59. https://doi.org/10.1007/s40641-015-0009-3

O'Neill, B. C., Tebaldi, C., Van Vuuren, D. P., Eyring, V., Friedlingstein, P., Hurtt, G., et al. (2016). The Scenario Model Intercomparison Project (ScenarioMIP) for CMIP6. *Geoscientific Model Development*, *9*(9), 3461–3482. https://doi.org/10.5194/gmd-9-3461-2016

Paik, S., & Min, S.-K. (2017). Climate responses to volcanic eruptions assessed from observations and CMIP5 multi-models. *Climate Dynamics*, *48*, 1017–1030. https://doi.org/10.1007/s00382-016-3125-4

Paik, S., Min, S.-K., Iles, C. E., Fischer, E. M., & Schure, A. P. (2020). Volcanic-induced global monsoon drying modulated by diverse El Niño responses. *Science Advances*, *6*(21), eaba1212. https://doi.org/10.1126/sciadv.aba1212

Santer, B. D., Bonfils, C., Painter, J. F., Zelinka, M. D., Mears, C., Solomon, S., et al. (2014). Volcanic contribution to decadal changes in tropospheric temperature. *Nature Geoscience*, *7*(3), 185–189. https://doi.org/10.1038/ngeo2098

Schneider, D. P., Ammann, C. M., Otto-Bliesner, B. L., & Kaufman, D. S. (2009). Climate response to large, high-latitude and low-latitude volcanic eruptions in the community climate system model. *Journal of Geophysical Research*, *114*, D15101. https://doi.org/10.1029/2008jd011222

Sigl, M., McConnell, J. R., Layman, L., Maselli, O., McGwire, K., Pasteis, D., et al. (2013). A new bipolar ice core record of volcanism from WAIS Divide and NEEM and implications for climate forcing of the last 2000 years. *Journal of Geophysical Research: Atmospheres*, *118*, 1151–1169. https://doi.org/10.1029/2012JD018603

Sigl, M., Winstrup, M., McConnell, J. R., Welten, K. C., Plunkett, G., Ludlow, F., et al. (2015). Timing and climate forcing of volcanic eruptions for the past 2,500 years. *Nature*, *523*, 543–549. https://doi.org/10.1038/nature14565

Stevenson, S., Otto-Bliesner, B., Fasullo, J., & Brady, E. (2016). "El niño like" hydroclimate responses to last millennium volcanic eruptions. *Journal of Climate*, *29*(8), 2907–2921. https://doi.org/10.1175/jcli-d-15-0239.1

Taylor, K. E., Stouffer, R. J., & Meehl, G. A. (2012). An overview of CMIP5 and the experiment design. *Bulletin of the American Meteorological Society*, *93*(4), 485–498. https://doi.org/10.1175/bams-d-11-00094.1

Timmreck, C. (2012). Modeling the climatic effects of large explosive volcanic eruptions. *Wiley Interdisciplinary Reviews-Climate Change*, *3*(6), 545–564. https://doi.org/10.1002/wcc.192

Trenberth, K. E., & Dai, A. (2007). Effects of mount pinatubo volcanic eruption on the hydrological cycle as an analog of geoengineering. *Geophysical Research Letters*, *34*(15), L15702. https://doi.org/10.1029/2007gl030524

van Vuuren, D. P., Edmonds, J., Kainuma, M., Riahi, K., Thomson, A., Hibbard, K., et al. (2011). The representative concentration pathways: An overview. *Climatic Change*, *109*, 5. https://doi.org/10.1007/s10584-011-0148-z

Wang, B., & Ding, Q. (2006). Changes in global monsoon precipitation over the past 56 years. *Geophysical Research Letters*, *33*(6), L0671. https://doi.org/10.1029/2005gl025347

Wang, B., Liu, J., Kim, H.-J., Webster, P. J., & Yim, S.-Y. (2012). Recent change of the global monsoon precipitation (1979-2008). *Climate Dynamics*, *39*(5), 1123–1135. https://doi.org/10.1007/s00382-011-1266-z

Wang, P., Wang, B., Cheng, H., Fasullo, J. T., Guo, Z., Kiefer, T., & Liu, Z. J. (2014). The global monsoon across timescales. *Coherent Variability of Regional Monsoons*, *10*(6), 2007–2052. https://doi.org/10.5194/cp-10-2007-2014

Wegmann, M., Brönnimann, S., Bhend, J., Franke, J., Folini, D., Wild, M., & Luterbacher, J. (2014). Volcanic influence on European summer precipitation through monsoons: Possible cause for "years without summer". *Journal of Climate*, *27*, 3683–3691. https://doi.org/10.1175/JCLI-D-13-00524.1

Yang, B., Zhang, Y., Qian, Y., Song, F., Leung, L. R., Wu, P., et al. (2019). Better monsoon precipitation in coupled climate models due to bias compensation. *npj Climate and Atmospheric Science*, *2*, 43. https://doi.org/10.1038/s41612-019-0100-x

Zambri, B., LeGrande, A. N., Robock, A., & Slawinska, J. (2017). Northern hemisphere winter warming and summer monsoon reduction after volcanic eruptions over the last millennium. *Journal of Geophysical Research: Atmospheres*, *122*, 7971–7989. https://doi.org/10.1002/2017JD026728

Zambri, B., & Robock, A. (2016). Winter warming and summer monsoon reduction aftervolcanic eruptions in Coupled Model Intercomparison Project 5 (CMIP5) simulations. *Geophysical Research Letters*, *43*(10), 10920–10928. https://doi.org/10.1002/2016GL070460

Zanchettin, D., Khodri, M., Timmreck, C., Toohey, M., Schmidt, A., Gerber, E. P., et al. (2016). The model intercomparison project on the climatic response to volcanic forcing (VolMIP): Experimental design and forcing input data for CMIP6. *Geoscientific Model Development*, *9*(8), 2701–2719. https://doi.org/10.5194/gmd-9-2701-2016

Zhang, H., & Delworth, T. L. (2018). Robustness of anthropogenically forced decadal precipitation changes projected for the 21st century. *Nature Communications*, *9*, 1150. https://doi.org/10.1038/s41467-018-03611-3

Zhang, W., Zhou, T., Zhang, L., & Zou, L. (2019). Future intensification of the water cycle with an enhanced annual cycle over global land monsoon regions. *Journal of Climate*, *32*(17), 5437–5452. https://doi.org/10.1175/jcli-d-18-0628.1

Zhuo, Z., Gao, C., Kirchner, I., & Cubasch, U. (2020). Impact of volcanic aerosols on the hydrology of the Asian monsoon and westerlies-dominated subregions: Comparison of proxy and multimodel ensemble means. *Journal of Geophysical Research: Atmospheres*, *125*, e2020JD032831. https://doi.org/10.1029/2020JD032831

Zuo, M., Zhou, T., & Man, W. (2019). Hydroclimate responses over global monsoon regions following volcanic eruptions at different latitudes. *Journal of Climate*, *32*(14), 4367–4385. https://doi.org/10.1175/jcli-d-18-0707.1